



Green Synthesis, Physicochemical, Optical and Antibacterial Activity Studies of Two Novel Organic Molecular Complexes of 2-Chloro-4-Nitrobenzoic Acid

Archana Pandey and B. Singh*

*Department of Chemistry, Centre of Advance study, Institute of Science,
Banaras Hindu University, Varanasi- 221005 INDIA

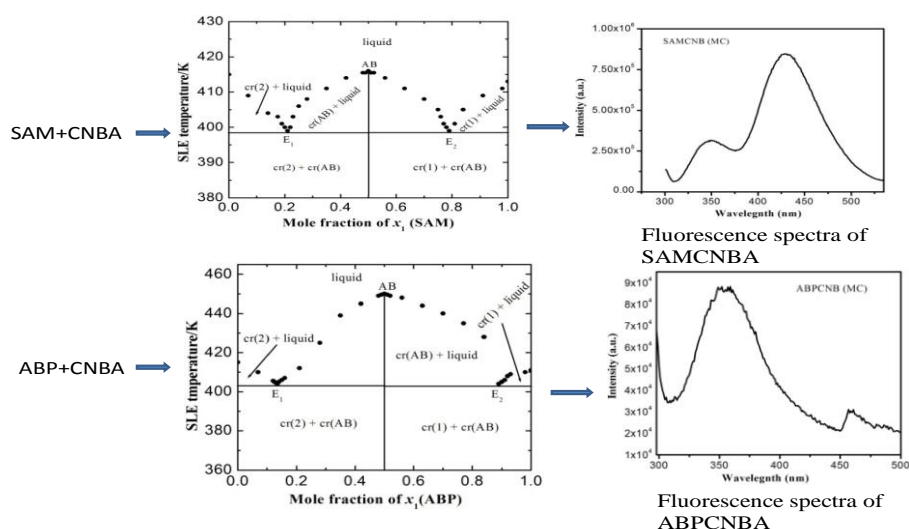
Email: bsinghbhu@rediffmail.com

Accepted on 2nd September 2017, Published online on 27th September 2017

ABSTRACT

Two novel organic complex compounds were synthesized via solid – liquid equilibrium investigation of organic systems; 2-chloro-4-nitrobenzoic acid – 2-hydroxybenzamide and 2-chloro-4-nitrobenzoic acid – 2-amino-5-bromopyridine and obtained their phase diagrams. In both the cases, their phase diagram study showed that the formation of a complex compound in 1:1 molar ratio with congruent melting temperature. The DSC Thermograms of SAMCNBA and ABPCNBA molecular complexes exhibited a melting temperature endotherm at 416 K and 451 K, respectively. The thermal behaviour of molecular complex has also been studied using TGA method. Spectral studies have supported the formation of complex compounds. The PXRD of SAMCNBA and ABPCNBA provide further support for formation of new compounds which are entirely different from their starting components. Both SAMCNBA and ABPCNBA are fluorescence. The excess thermodynamic functions have been computed. The antibacterial study of both the materials has been shown moderate bacterial growth inhibition activity. SAMCNBA shows the good antibacterial activity against *E. Feacalis* and *P. fluorescence* bacteria.

Graphical Abstract:



Highlights

- Two novel organic molecular complexes (SAMCNBA and ABPCNBA) have been synthesized.
- Both molecular complexes have been formed in 1:1 molar ratio of its component.
- Melting point of SAMCNBA and ABPCNBA have been found 416 K and 451 K, respectively.
- SAMCNBA and ABPCNBA complexes show the better emission properties.
- SAMCNBA and ABPCNBA show the good antibacterial activity against the growth of gram positive bacteria *E. faecalis*, MIC values $12.20 \mu\text{g mL}^{-1}$.
- SAMCNBA shows the good antibacterial activity against both gram positive bacteria (*E. faecalis*) and gram negative (*P. fluorescens*).

Keywords: Solid- liquid equilibrium, thermal property, powder X-ray diffraction, optical property, antibacterial activity.

INTRODUCTION

The investigation of solid – liquid of organic systems has significant importance in the field of materials. In last few decades, organic materials with aromatic ring skeleton have attracted much attention due to their various promising properties such as optical [1-4] and non linear optical (NLO) [5-6] properties. Organic materials are used in numerous applications such as organic light emitting diodes (OLEDs) [3,4,7,8], organic solar cells and many more due to their light weight, solubility, low temperature processability, high yield and low cost. The organic materials have given rise to numerous potential applications for the development of manifold devices like electronic [9-10] optoelectronic [11]. Formation of molecular complexes is easily possible due to intermolecular hydrogen bonding interaction between the molecules of different organic compounds. These materials form an important class of compounds because they are able to control the properties such as physicochemical and pharmaceutical of new compounds without changing in the bonding of parent compounds.

Salicylamide has medicinal uses similar to aspirin and known to be a non-prescribed drug with analgesic, antipyretic and anti-inflammatory properties [12]. In addition, hydroxybenzamides are also used as non-active pharmaceutical components to design co-crystals which help to improve the solubility of the active pharmaceutical ingredient. 2-chloro-4-nitrobenzoic acid, an active pharmaceutical ingredient has been potentially used in novel therapy for immunodeficiency (HIV) diseases as an antiviral and anticancer agent [13-14] and has ability to participate as acidic donor and has maximum possibility of intermolecular hydrogen bonding interactions with the acceptor component. As we know that aminopyridine and its derivatives are also an important class of compounds that is why these compounds are used as starting components to synthesize the new molecular complex in our study. Large number of pyridines and amides co-crystallize with aromatic acid derivatives reported in the literature [15-22].

Herein, we report the synthesis of two novel organic complex compounds via phase diagram analysis. The materials were characterized using several techniques such as by FTIR, NMR, DSC, TGA methods. UV-Vis absorption and emission as well as powder X-ray diffraction studies have also been performed. To study antibacterial activity of both molecular complexes, these were screened against *Staphylococcus aureus*, *Enterococcus faecalis* and *Pseudomonas fluorescens* bacterial strains.

MATERIALS AND METHODS

Chemicals: The starting chemicals namely, 2-hydroxybenzamide (Salicylamide) 98%, 2-chloro-4-nitrobenzoic acid 98% and 2-amino-5-bromopyridine 98% were received from Sigma-Aldrich, Germany. The materials were employed as received. The melting temperature of 2-hydroxybenzamide, 2-chloro-4-

nitrobenzoic acid, 2-amino-5-bromopyridine were determined using DSC method. The purity of each component was assessed by comparing their melting temperatures with literature values.

Phase diagram study: The solid – liquid equilibrium of Salicylamide (1) – 2-chloro-4-nitrobenzoic acid (2) (SAM – CNBA) and 2-amino-5-bromopyridine (1) – 2-chloro-4-nitrobenzoic acid (2) (ABP – CNBA) systems have been studied and their phase diagrams were obtained by using the traditional thaw-melt method [23-24]. To prepare the series of solid binary organic mixtures of different compositions covering the entire compositional range, the pure components were weighed using a four digit electronic balance (Denver SI-234, Germany with accuracy ± 0.0002 g). Each binary mixture was taken in separate clean glass test tube and the mouth of each test tube was sealed to prevent the environmental effect. The silicone oil bath was maintained at about 5.0 °C above the melting temperature of higher melting component present in the mixture, the mixtures were melted and homogenized properly followed by chilling in ice cooled water. The process was repeated 3-4 times. The resultant materials were powdered using a clean mortar-pestle. The melting temperatures of all the synthesized powdered materials were determined by using a melting point apparatus (Toshniwal melting point apparatus) attached with a thermometer which could read up to ± 0.5 °C. During the melting temperature determination, the heating rate was kept slow i.e. $3\text{--}4$ °C per minute. A graph was plotted between melting temperatures and composition on y-axis and x-axis, respectively.

Thermal Study (DSC and TGA): To determine the melting temperature and heat of fusion values of synthesized complexes, parent components as well as their eutectics, differential scanning calorimeter (DSC) was used. DSC profile was generated using Mettler DSC-4000 system. Temperature calibration was performed by using indium metal as the standard. The test samples were accurately measured, $4\text{--}6$ mg were taken in aluminium pan and an empty pan was used as reference and heating rate was maintained at 10 °C min^{-1} . The values of enthalpy of fusion were found reproducible within ± 0.01 kJ mol^{-1} . The samples were purged with a stream of flowing nitrogen throughout the experiment. Thermal stability of the synthesized molecular complexes was studied by thermo gravimetric analysis (TGA) method. TGA was performed using a Perkin-Elmer STA 6000 thermal analyser in the temperature range from 30 to 500 °C and the heating rate was 10 °C/min. The samples were purged with a stream of flowing nitrogen throughout the experiment.

IR and NMR: IR spectroscopy is an important spectroscopic tool to distinguish and characterize hydrogen bonds because the vibrational modes are sensitive towards these types of interactions. The FTIR spectra of Salicylamide, 2-chloro-4-nitrobenzoic acid, 2-amino-5-bromopyridine and complex compounds have been recorded in the region $4000\text{--}400$ cm^{-1} using a Perkin Elmer FT-IR Spectrum, 1000 Infrared Spectrometer at the room temperature. The test samples were pelletized in KBr. ^1H and ^{13}C NMR spectra of SAM (1) – CNBA (2) system were recorded in the in CDCl_3 while ABP (1) – CNBA (2) system recorded in DMSO as solvent, respectively, using JEOL AL300 MHz Spectrometer.

Powder X-ray diffraction: Powder X-ray diffraction patterns were recorded for the starting chemicals, molecular complexes and their eutectics (E_1 and E_2) using an 18 kW rotating (Cu) anode based Rigaku powder diffractometer fitted with a graphite monochromator in the diffracted beam. The samples were scanned from 10° to 70° with a scanning rate of 4° min^{-1} .

Optical study (UV-Vis absorption and Emission): UV-Vis absorption spectra of complex compounds as well as starting compounds were recorded using JASCO V-670 absorption spectrophotometer in the region ($900\text{--}200$ nm) in methanol solvent. Emission study of both the molecular complexes was performed and recorded using Varian Cary Eclipse Fluorescence Spectrophotometer in solution medium.

Antibacterial studies: The newly prepared molecular complexes were screened for their antibacterial activity against *Staphylococcus aureus*, *Enterococcus faecalis* and *Pseudomonas florescence* by dropping

the samples each on a cultured sterile plate. The medium used in the experiment was prepared as: MHA (Mueller Hinton Agar) 3.8% MHA and 1% agar powder and composition of MHA (Meat in fusion form 300gL^{-1} , Casein acid hydrolysate 17.50gL^{-1} , Starch 1.50gL^{-1} , Agar 17.00gL^{-1}) in conical a flask and made sterile by autoclaving. The petri glass plates were sterilised in a hot air oven. 20 mL prepared media was poured in each plate in 90 mm diameter and waited for the media solidification after that the minimum inhibitory concentration (MIC) of compounds was determined by dilution method. The sample compounds were dissolved in fixed volume of DMSO solvent and diluted it serially with two fold dilution factor in each dilution step. The lawn of bacteria is prepared in bacterial suspension of 0.5 Mac Fernald number (1.5×10^8 cfu). The plats were incubated at 37°C for 2 h and dropped each dilution on plates and culture was incubated again overnight and growth was monitored visually.

RESULTS AND DISCUSSION

Phase diagram: The experimental phase diagrams of both the systems namely, Salicylamide (1) – 2-chloro-4-nitrobenzoic acid (2) and 2-amino-5-bromopyridine (1)–2-chloro-4-nitrobenzoic acid (2) established by the melting temperature-compositions curves, have been shown in figs.1a, b, respectively. In both the cases molecular complex has formed at 1:1 molar ratio and each complex having congruent melting temperature. In the diagram of Salicylamide (1) – 2-chloro-4-nitrobenzoic acid (2) system, two eutectics E_1 and E_2 are found at 0.210 and 0.790 mole fraction of Salicylamide (SAM), respectively, and melting temperature of both eutectics are 399.0 K. On the other hand in the phase equilibrium diagram of 2-amino-5-bromopyridine (1) – 2-chloro-4-nitrobenzoic acid (2) system, eutectics E_1 and E_2 are observed at 0.135 and 0.890 mole fraction of 2-amino-5-bromopyridine (ABP) component and melting temperature is 404.0 K in both the cases.

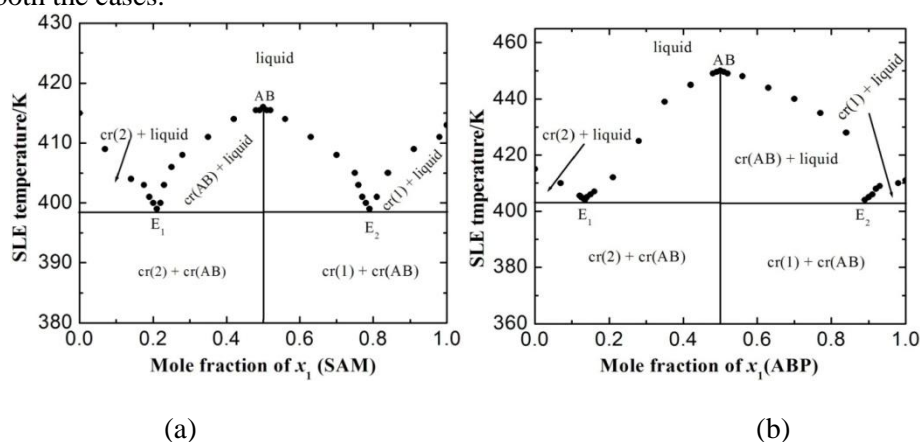


Fig 1. Phase diagram of a) Salicylamide (1) – 2-chloro-4-nitrobenzoic acid (2) system and b) 2-amino-5-bromopyridine (1) – 2-chloro-4-nitrobenzoic acid (2) system

Thermal study: The DSC curves of Salicylamide (1) – 2-chloro-4-nitrobenzoic acid (2) and 2-amino-5-bromopyridine (1) – 2-chloro-4-nitrobenzoic acid (2) systems have been shown in Figs. 2 a ,b. Both SAMCNBA and ABPCNBA complexes exhibit the melting endotherm maximum at 416 K and 451K, respectively. DSC data provided support for the formation of new complexes. The thermal behaviour of the new complex compounds is significantly different from their constituents. Furthermore, thermal parameters have been computed using DSC data, the experimental enthalpy of fusion and values that is computed using mixture law have been given in Table 1. The enthalpy of mixing values are found negative in each eutectic of SAM (1) – CNBA (2) system and E_1 of ABP (1) – CNBA (2) system which suggest clustering of molecules [25]. E_2 of the second system shows the positive enthalpy of mixing which indicated the quasi eutectic nature and its enthalpy of mixing values have been reported in Table 1. The excess thermodynamic function calculated by using equations as earlier [26],

$$g^E = RT \left[x_1 \ln \gamma_1^l + x_2 \ln \gamma_2^l \right] \quad (1)$$

$$h^E = -RT^2 \left[x_1 \frac{\partial \ln \gamma_1^l}{\partial T} + x_2 \frac{\partial \ln \gamma_2^l}{\partial T} \right] \quad (2)$$

$$s^E = -R \left[x_1 \ln \gamma_1^l + x_2 \ln \gamma_2^l + x_1 T \frac{\partial \ln \gamma_1^l}{\partial T} + x_2 T \frac{\partial \ln \gamma_2^l}{\partial T} \right] \quad (3)$$

where, $\ln \gamma_i^l$, x_i and $\frac{\ln \gamma_i^l}{\partial T}$ are activity coefficient in the liquid state, the mole fraction and the variation of log of activity coefficient in liquid state as a function of temperature of the component i, 1 and 2. It is evident from Eqs. 1-3, that activity coefficient and its variation with temperature is required to calculate the excess functions. Activity coefficient (γ_i^l) could be evaluated using the following equation [26],

$$-\ln(x_i \gamma_i^l) = \frac{\Delta_{fus} H_i}{R} \left(\frac{1}{T_{fus}} - \frac{1}{T_i} \right) \quad (4)$$

where, x_i , $\Delta_{fus} H_i$, T_i and T_{fus} are mole fraction, enthalpy of fusion, melting temperature of component i and melting temperature of eutectics, respectively. The variation of activity coefficient with temperature could be calculated by differentiating Eq. 5 with respect to temperature,

$$\frac{\partial \ln \gamma_i^l}{\partial T} = \frac{\Delta_{fus} H_i}{RT^2} - \frac{\partial x_i}{x_i \partial T} \quad (5)$$

where, $\partial x_i / \partial T$ in this expression can be evaluated by considering two nearest points of eutectic. The positive value of excess free energy in all the eutectics in both the investigated systems indicated that an association between like molecules are stronger than that of unlike molecules. Roughness parameters were also calculated using reported equations [26].

$$\alpha = \xi \Delta_{fus} H / RT \quad (6)$$

where ξ is the crystallographic factor, generally ($\xi \leq 1$). When $\alpha > 2$, crystals develop with a faceted morphology and interface will be relatively smooth while $\alpha < 2$, crystals grow with non-faceted morphology and interface surface will be rough. In this study, the value of $\alpha > 2$ in all the cases, the calculated values of roughness parameters have been given in table 3.

However, the interfacial energy (σ) [25] is given by

$$\sigma = \frac{C \Delta_{fus} H}{(N_A)^{1/3} (V_m)^{2/3}} \quad (7)$$

where, N_A is the Avogadro Number, V_m is the molar volume, and parameter C lies between 0.30 to 0.35. The value of C (0.35) was used for calculation. The interfacial energy of the samples was calculated using Eq. 7. The excess thermodynamic functions of eutectics are reported in Table 2 while interfacial energy of starting components molecular complexes and their eutectics has been reported in table 3.

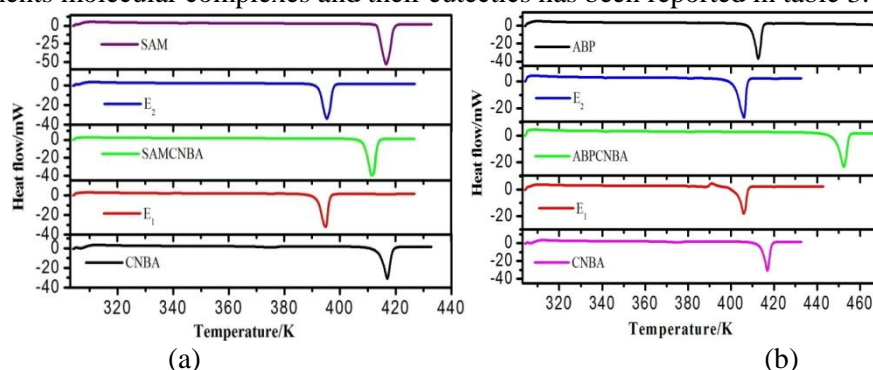


Fig 2. DSC curves of a) SAM (1) – CNBA (2) and b) ABP (1) – CNBA (2) system

Table 1. Enthalpy of fusion, heat of mixing and entropy of fusion of starting materials, SAMCNBA and ABPCNBA molecular complexes, and their eutectics

| S. No. | Materials | Enthalpy of fusion (kJ mol ⁻¹) | Heat of mixing (kJ mol ⁻¹) | Entropy of fusion (kJ mol ⁻¹ K ⁻¹) |
|--------|------------------------------------|--|--|---|
| 1. | SAM | 25.55 | | 0.062 |
| 2. | CNBA | 23.82 | | 0.057 |
| 3. | E ₁ (Exp.) (Cal.) | 31.40 37.02 | -5.62 | 0.079 |
| 4. | E ₂ (Exp.) (Cal.) | 29.35 38.07 | -8.67 | 0.073 |
| 5. | SAMCNBA (MC) (Exp.) (Cal.) | 55.25 24.68 | 30.57 | 0.133 |
| 6. | ABP | 25.99 | | 0.063 |
| 7. | E ₁ (Exp.) (Cal.) | 22.48 30.68 | -8.20 | 0.055 |
| 8. | E ₂ (Exp.) (Cal.) | 31.65 31.10 | 0.55 | 0.078 |
| 9. | ABPCNBA(MC) (Exp.) (Cal.) | 49.23 24.90 | 24.33 | 0.109 |

Table 2. Excess free energy (g^E), excess enthalpy (h^E) and excess entropy (s^E) of eutectics of Salicylamide (1) – 2-chloro4-nitrobenzoic acid (2) and 2-amino-5-bromopyridine (1) – 2-chloro-4-nitrobenzoic acid (2) systems

| S.N. | System | g^E (kJ mol ⁻¹) | h^E (kJ mol ⁻¹) | s^E (kJ mol ⁻¹ K ⁻¹) |
|------|-------------------|-------------------------------|-------------------------------|---|
| 1. | SAM (1) – CNBA(2) | | | |
| | E ₁ | 0.8296 | -7.7430 | -0.0215 |
| | E ₂ | 0.1766 | -8.7796 | -0.0224 |
| 2. | ABP (1) – CNBA(2) | | | |
| | E ₁ | 0.1923 | -13.64 | -0.0341 |
| | E ₂ | 0.3734 | -11.59 | -0.0295 |

Table 3. Interfacial energy and roughness parameters of SAM, CNBA, ABP, molecular complexes and their eutectics

| Compounds | Interfacial Energy (erg cm ⁻²) | Roughness parameter |
|------------------------|--|---------------------|
| σ_{SL_1} (SAM) | 48.15 | 7.4214 |
| σ_{SL_2} (CNBA) | 39.32 | 6.9040 |
| E ₁ | 41.74 | 9.4660 |
| E ₂ | 46.30 | 8.8285 |
| SAMCNB(MC) | 43.74 | 16.0091 |
| σ_{SL_1} (ABP) | 49.56 | 7.578 |
| E ₁ | 40.70 | 6.615 |
| E ₂ | 48.43 | 9.382 |
| ABPCNB (MC) | 44.44 | 13.110 |

TGA plots of SAMCNBA and ABPCNBA molecular complexes have been shown in figs. 3a,b. SAMCNBA molecular complex shows the thermal stability up to 450K i.e. it is stable after melting and ABPCNBA is thermally stable up to 452K, it is thermally more stable than that of its constituents.

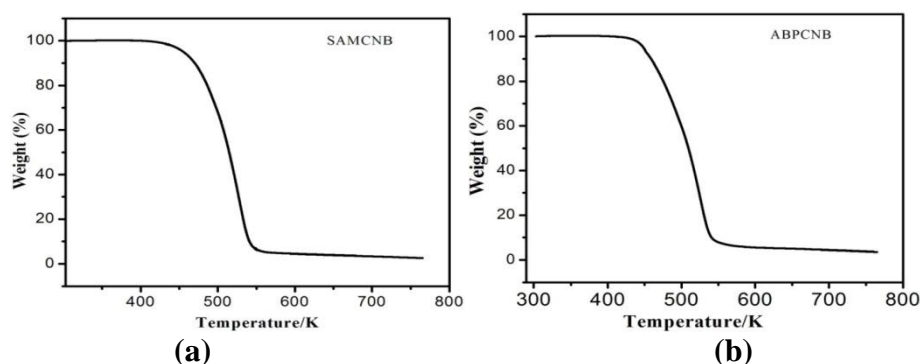


Fig 3. TGA plot of a) SAMCNBA and b) ABPCNBA molecular complexes

FT-IR and NMR: In case of SAM(1) – CNBA(2) system, FT-IR spectra have been shown in Fig. 4 (a). FT-IR spectrum of CNBA [13] shows a peak in the region $3100\text{--}2500\text{ cm}^{-1}$ due to --OH stretching and a peak appears at 1712 cm^{-1} due to --C=O of --COOH group of CNBA. A peak appears at 1690 cm^{-1} due to --C=O of amide of SAM [27], it shifted at 1688 cm^{-1} in IR spectrum of the complex, it confirmed that the amide carbonyl participates in the hydrogen bonding with the CNBA and --OH stretching region also shifts towards lower wave number in the molecular complex spectrum.

In case of ABP (1) – CNBA (2) system, spectra have been shown in Fig. 4 (b). IR spectrum of CNBA peak appears at 3100 cm^{-1} due to stretching of O--H of carboxylic acid and it shifts at 3089 cm^{-1} in the spectrum of the complex due to the involvement of acid proton in formation of pyridinium ion. FT-IR of ABPCNBA molecular complex shows a peak at 1659 cm^{-1} due to bending mode of pyridinium ion and a peak at 1579 cm^{-1} due to stretching of C=N of pyridine ring. The IR vibrational peak at 3325 cm^{-1} of --NH_2 group of the ABP [28] pyridine ring remains unaffected. The vibrational data show hydrogen bonding nature of studied complexes.

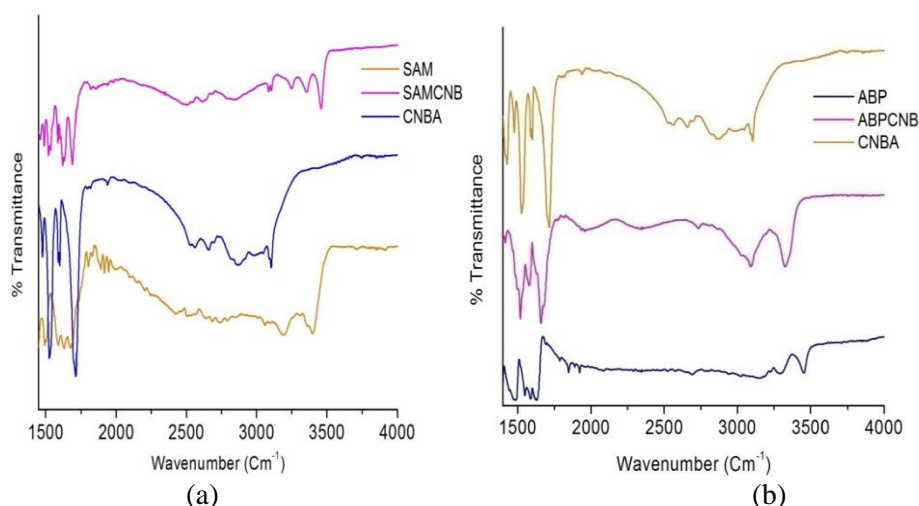


Fig 4. FT-IR spectra of a) SAM (1) – CNBA (2) and b) ABP (1) – CNBA (2) systems

In case of SAM (1) – CNBA (2) system, proton NMR spectrum of SAMCNBA molecular complex shows peaks at (1H, d) 8.14 ppm, (1H, d) 8.20 ppm, (1H, s) 8.31 ppm, (1H, d) 7.40 ppm, (1H, t) 7.47 ppm, (1H, t) 6.91 ppm, (1H, d) 7.02 ppm due to aromatic ring protons. The signal at 6.51 ppm (2H, s) due to the --NH_2 proton of SAM amide group has involved in the intermolecular hydrogen bonding with --COOH group of

CNBA parent. In the proton NMR spectrum of CNBA, $-\text{COOH}$ proton appears at 11 ppm and it shifts to 11.83 ppm in the proton NMR spectrum of complex, indicates that the acidic proton of CNBA are actively involved in hydrogen bonding. The above results strongly supported the complex formation and both the parent components are involved in 1:1 molar ratio.

In ^{13}C NMR spectrum of complex, a peak appears at 170.65 ppm due to presence of $-\text{COOH}$ group of CNBA, a peak at 159.96 ppm due to amide carbon of SAM.

In ABP (1) – CNBA (2) system, proton NMR spectrum of complex, peaks appears at (1H, d) 6.42 ppm, (1H, d) 7.49 ppm, (1H, s) 7.93 ppm, (1H, s) 8.34 ppm, (1H, d) 7.99 ppm and (1H, d) 8.24 ppm due to the aromatic ring protons. The $-\text{NH}_2$ protons of ABP appeared at (2H, s) 6.14 ppm. The acidic $-\text{COOH}$ proton of CNBA appears at 11 ppm in the NMR spectrum of CNBA and it shifts to 11.83 ppm in the complex spectrum.

In the ^{13}C NMR spectrum of complex, peaks appeared at 104.98 ppm, 110.04 ppm, 114.04 ppm, 122.26 ppm, 125.25 ppm, 131.36 ppm, 137.74 ppm, 139.19 ppm, 147.63 ppm, 155.68 ppm, 168.18 ppm due to the aromatic ring carbon. The peak at 186.79 ppm in the spectrum of complex compound is due to carboxylic carbon of CNBA. On the basis of proton NMR and ^{13}C NMR data, we could conclude that the formation of complex compound occurs at 1:1 molar ratio of parent components and also that in the formation of complex compound, hydrogen bonding may take place between pyridine group of ABP and acidic group of CNBA. ^1H and ^{13}C NMR support the formation of molecular complex in 1:1 ratio because the total number of proton and carbon present in the NMR spectrum of the molecular complex.

Powder XRD Analysis: The powder XRD patterns of molecular complexes of both the systems from Figs. 5 a, b are clearly different from those of starting components and confirming the crystalline phase of the novel materials. PXRD patterns [29] inform about the entirely different nature of the materials. In case of SAM (1) – CNBA (2) system, X-ray diffraction pattern of molecular complex is different from its constituents and several new peaks appear which indicates that synthesized molecular complex is a new compound while in case of eutectics, E_1 shows the peaks of molecular complex and CNBA whereas E_2 shows the diffraction peaks of SAM as well as molecular complex. Similarly, in case of ABP (1) – CNBA (2) system, molecular complex shows various new diffraction peaks and intensity of several peaks are significantly changes from its constituents. These changes indicate that the molecular complex is entirely new in nature and eutectic E_1 shows the peaks of CNBA and molecular complex while E_2 shows the diffraction peaks of ABP and molecular complex.

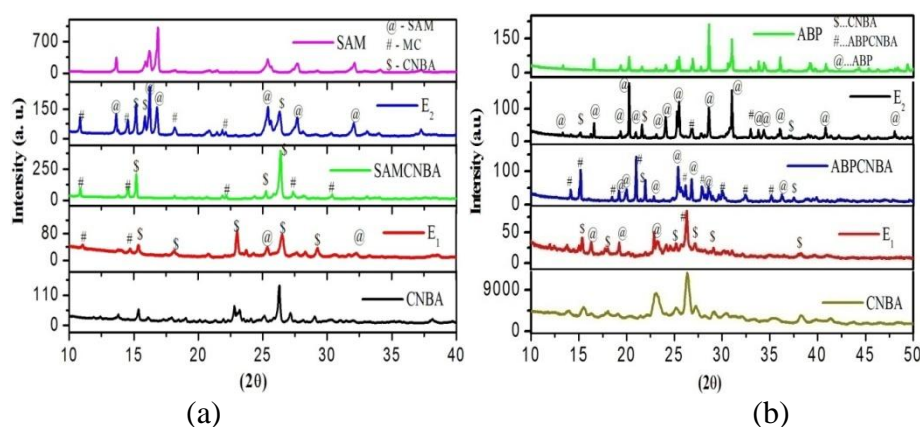


Fig 5. Powder X-ray diffraction patterns of a) SAM (1) – CNBA (2) and b) ABP (1) – CNBA (2) systems

Optical study (UV-Vis absorption and Emission): In case of SAM (1) – CNBA (2) system, UV-Vis absorption spectra have been shown in Fig. 6(a), the absorption spectra of Salicylamide (SAM), show two bands at 235 nm, 302 nm due to $n \rightarrow \pi^*$ transition. The band at 235 nm appears due to amide group of SAM, and amide ($>C=O$) group involved in the hydrogen bonding due to which band slightly shifts and appears at 241 nm in the complex spectrum due to $\pi \rightarrow \pi^*$ transition. The absorption spectrum of 2-chloro-4-nitrobenzoic acid (CNBA) shows two bands one higher energy band at 206 nm due to $n \rightarrow \sigma^*$ transition and another band at 281 nm due to the $n \rightarrow \pi^*$ transitions which due to the presence of non bonded electrons of $-COOH$ group, the more acidic proton of CNBA involves in the inter molecular hydrogen bonding to other component (SAM), due to which non bonded electron of CNBA slightly involved in bonding, it shows bathochromic shifts and appears at 295 nm due to the $n \rightarrow \pi^*$ transitions in the complex spectrum. On the basis of these results we could conclude that molecular complex formation occurs by inter molecular hydrogen bonding between Salicylamide (SAM) and 2-chloro-4-nitrobenzoic acid (CNBA) components.

In ABP (1) – CNBA (2) system, spectra have been shown in fig. 6 (b), UV-vis absorption spectrum of 2-amino-5-bromopyridine (ABP) shows a band at 243 nm which would be assigned to $\pi \rightarrow \pi^*$ transition with aromatic ring and a second band at 313 nm due to $n \rightarrow \pi^*$ transition within ($-C=N-$) the pyridine nitrogen and ring carbon which has been ascribed as absorption maxima. In case of CNBA, a band appears at 281 nm due to the $n \rightarrow \pi^*$ transition within $-COOH$ group which is the λ_{max} absorption. In the UV-Vis absorption spectrum of complex λ_{max} absorption band appears at 286 nm which has blue shifted with 27 nm as compared to ABP λ_{max} absorption while slightly red shifted about 6 nm as compared to CNBA λ_{max} absorption. On the basis of these observations, it has been concluded that the acid group of 2-chloro-4-nitrobenzoic acid (CNBA) shows inter molecular hydrogen bonding interaction with the pyridine nitrogen of 2-amino-5-bromopyridine (ABP) resulting in a new molecular complex.

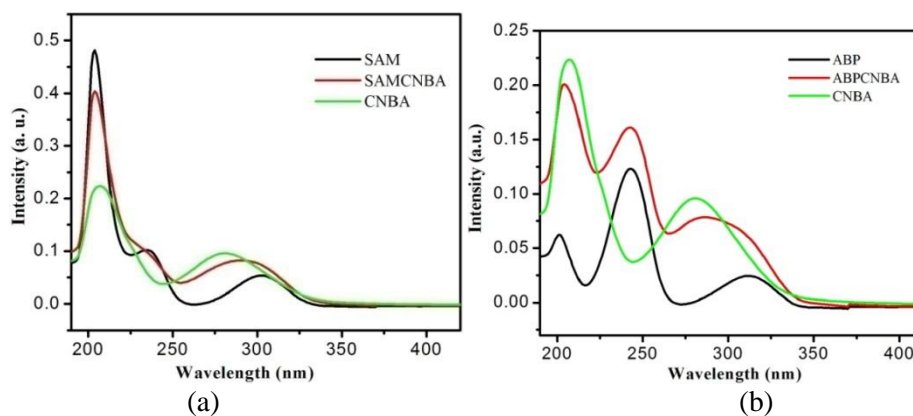


Fig. 6: UV-Vis absorption spectra of **a)** SAM (1) – CNBA (2) system and **b)** ABP (1) – CNBA (2) system

The emission behaviour of synthesized complexes was studied and spectrum has been shown in figs.7 a, b. SAMCNB molecular complex shows the dual emission band at its λ_{max} excitation, first band has appeared at 310 nm to 370 nm and second emission band at 380 nm to 530 nm with higher intensity than that of the first band. On the other hand ABPCNB molecular complex shows emission band at 310 nm to 450 nm. SAMCNBA molecular complex shows the better emission than ABPCNBA complex.

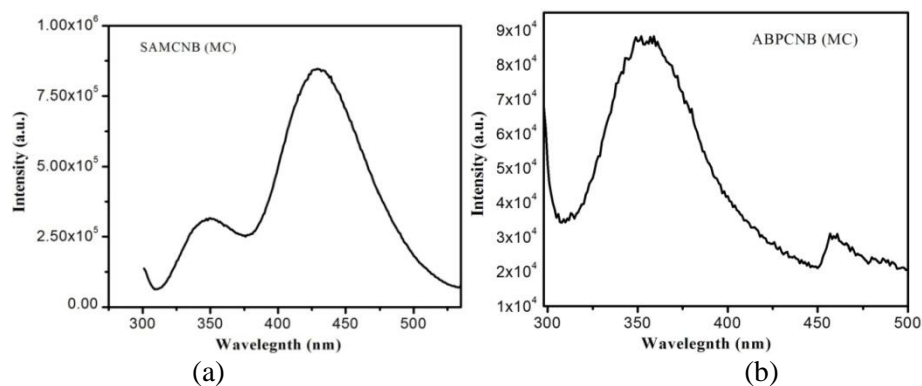


Fig. 7: Emission spectra of a) SAMCNBA and b) ABPCNBA molecular complexes

Antibacterial studies: The antibacterial activity of synthesized materials has been studied against *Staphylococcus aureus*, *E. faecalis* and *pseudomonas florescence bacterial strain* [30]. The minimum inhibitory concentration (MIC) of the samples has been reported in table 4. The investigation of screened antibacterial data reveals that both the complexes show good antibacterial activity [31-35] against *E. faecalis* bacteria while in case of *Staphylococcus aureus Pseudomonas florescence* the moderate bacterial inhibition is exhibited. SAMCNBA shows the good antibacterial activity against *Pseudomonas florescence*.

Table 4. Minimum inhibitory concentration (MIC in $\mu\text{g/ml}$) of SAMCNBA and ABPCNBA molecular complexes

| S. No. | Sample name | <i>E. faecalis</i> | <i>P. florescence</i> | <i>S. aureus</i> |
|--------|-------------|--------------------|-----------------------|------------------|
| 1. | SAMCNBA | 12.20 | 24.41 | 48.82 |
| 2. | ABPCNBA | 12.20 | 48.82 | 48.82 |

APPLICATIONS

Both SAMCNBA and ABPCNBA compounds show good fluoresce. Antibacterial activity have been studied, both are showing good inhibition activity against *E. faecalis* at MIC 12.20 $\mu\text{g/ml}$ and moderate against *S. aureus* and *P. florescence*.

CONCLUSIONS

The phase equilibrium investigations of selected systems confirmed the compositional details of synthesized molecular complexes, both in 1:1 molar ratio of their constituents. A complete thermal study performed by DSC and TG reveals that ABPCNBA molecular complex is stable in their solid form and thermally more stable than that of its constituents. Melting temperatures of SAMCNBA and ABPCNBA are 416 K and 451 K, respectively. The FTIR spectral analysis helped that hydrogen bonding interactions are involved in the formation of complexes. Both the molecular complexes are entirely of different nature from their constituents which is confirmed by X-ray powder diffraction pattern. UV-Vis absorption analysis of both the complexes suggests that new absorption, Emission study reveals that both the complexes show emission at their λ_{max} excitation while SAMCNBA shows the better emission behaviour with higher intensity than ABPCNBA complex. The minimum inhibitory concentration (MIC) of synthesized compounds was studied. The investigation of screened antibacterial data reveals that the tested samples showed good antibacterial inhibition. SAMCNBA shows the good antibacterial activity against both gram positive (*E. faecalis*) and gram negative (*P. florescence*).

ACKNOWLEDGEMENTS

The authors gratefully acknowledge the financial support of the UGC, New Delhi, through BSR scheme and Head, department of chemistry, B.H.U. for infrastructural facility and Prof. G. Nath (Department of Microbiology, Institute of Medical Sciences, B.H.U.) for antibacterial activity study.

REFERENCES

- [1] E. Gondek, I.V. Kityk, J. Sanetra, P. Szlachcic, P. Armatys, A. Wisla, A. Danel, New-synthesized pyrazoloquinoline as promising luminescent materials, *Optics & Laser Technology.*, **2006**, 38, 487–492.
- [2] G. Hughes, M. R. Bryce, Electron-transporting materials for organic electroluminescent and electro phosphorescent devices, *J. Mater. Chem.*, **2005**, 15, 94–107.
- [3] B. Geffroy, P. L. Roy, Prat, C., Organic light-emitting diode (OLED) technology: materials, devices and display technologies, *Polym. Int.*, **2006**, 55, 572–582.
- [4] S. Reineke, F. Lindner, G. Schwartz, N. Seidler, K. Walzer, B. Lussem, K. Leo, White organic light-emitting diodes with fluorescent tube efficiency, *NATURE*, **2009**, 459, 234–238.
- [5] R. O. Priakumari, S. G. S. Sheba, M. Gunasekaran, Synthesis, growth and characterization of non-linear optical material: L-Tryptophan p-nitrophenol (LTPNP) single crystal, *Optik.*, **2014**, 125, 4633–4636.
- [6] O. P. Kwon, S. J. Kwon, M. Jazbinsek, A. Choubey, V. Gramlich, P. Gunter, New Organic Nonlinear Optical Polyene Crystals and Their Unusual Phase Transitions, *Adv. Funct. Mater.*, **2007**, 17, 1750–1756.
- [7] Y. Karzazi, Organic Light Emitting Diodes: Devices and applications, *J. Mater. Environ. Sci.*, **2014**, 5, 1–12.
- [8] C.-T. Chen, Evolution of Red Organic Light-Emitting Diodes: Materials and Devices, *J. Chem. Mater.*, **2004**, 16, 4389–4400.
- [9] B. Z. Bao, Materials and Fabrication Needs for Low-Cost Organic Transistor Circuits, *Adv. Mater.*, **2000**, 12 3, 227–230.
- [10] J. Godlewski, M. Obarowska, Application of organic materials in electronics, *Eur. Phys. J. Special Topics.*, **2007**, 144, 51–66.
- [11] S. R. Forrest, M. E. Thompson, Introduction: Organic Electronics and Optoelectronics, *Chem. Reviews.*, **2007**, 107 (4), 923–925.
- [12] A. N. Manin, A. P. Voronin, G. L. Perlovich, Thermodynamic and structural aspects of hydroxybenzamide molecular crystals study, *Thermochim. Acta.*, **2013**, 551, 57–61.
- [13] I. Barsky, J. Bernstein, P. W. Stephens, K. H. Stone, The study of the polymorphic system of 2-chloro-4-nitrobenzoic acid, *New J. Chem.*, **2008**, 32, 1747–1753.
- [14] S. Aitipamula, P. S. Chow, B. H. T. Reginald, Solvates and polymorphic phase transformations of 2-chloro-4-nitrobenzoic acid, *Cryst Eng Comm.*, **2011**, 13, 1037–1045.
- [15] Lemmerer, C. Esterhuysen, J. Bernstien, Synthesis, Characterization, and Molecular Modeling of a Pharmaceutical Co-Crystal: (2-Chloro-4-Nitrobenzoic Acid):(Nicotinamide), *J. Pharm. Sci.*, **2010**, 99, 4054–4071.
- [16] M. A. Elbagerma, H. G. M. Edwards, T. Munshi, I. J. Scowen, Identification of a new co-crystal of salicylic acid and benzamide of pharmaceutical relevance, *J. Anal Bioanal Chem.*, **2010**, 397, 37–146.
- [17] J. I., A. Garcia, D. H. Ruiz, K. M. Vasquez, H. M. Rojas, H. Hopf, dx.doi.org/10.1021/cg201140g, Modification of the Supramolecular Hydrogen-Bonding Patterns of Acetazolamide in the Presence of Different Cocrystal Formers: 3:1, 2:1, 1:1, and 1:2 Cocrystals from Screening with the Structural Isomers of Hydroxybenzoic Acids, Aminobenzoic Acids, Hydroxybenzamides, Aminobenzamides, Nicotinic Acids, Nicotinamides, and 2,3-Dihydroxybenzoic Acids, *Cryst. Growth Des.*, **2012**, 12 , 811–824.

- [18] S. Aitipamula, A. B. H. Wong, P. S. Chow, B. H. Tan Reginald, Pharmaceutical cocrystals of ethenzamide: structural, solubility and dissolution studies, *Cryst Eng Comm.*, **2012**, 14, 8515–8524.
- [19] Y.-H. Luo, B.-W. Sun, Co-crystallization of pyridine-2-carboxamide with a series of alkyl dicarboxylic acids with different carbon chain: Crystal structure, spectroscopy and Hirshfeld analysis, *Spectrochimica Acta Part A: Molecular and Biomolecular Spectroscopy.*, **2014**, 120, 228–236.
- [20] B.-W. Y.-H. Luo, Sun, dx.doi.org/10.1021/cg400167w | Pharmaceutical Co-Crystals of Pyrazine carboxamide (PZA) with Various Carboxylic Acids: Crystallography, Hirshfeld Surfaces, and Dissolution Study, *Cryst. Growth Des.*, **2013**, 13, 2098–2106.
- [21] N. Manin, A. P. Voronin, N. G. Manin, M. V. Vener, A. V. Shishkina, A. S. Lermontov, G. L. Perlovich, Salicylamide Cocrystals: Screening, Crystal Structure, Sublimation Thermodynamics, Dissolution, and Solid-State DFT Calculations, *J. Phys. Chem. B.*, **2014**, 118, 6803–6814.
- [22] C. B. Aakeroy, A. Li Z. J. Rajbanshi, , D. John, Mapping out the synthetic landscape for recrystallization, co-crystallization and salt formation, *Cryst. Eng. Comm.*, **2010**, 12, 4231–4239.
- [23] T. Agrawal, P. Gupta, S. S. Das, A. Gupta, N. B. Singh, Phase Equilibria, Crystallization, and Microstructural Studies of Naphthalen-2-ol + 1,3-Dinitrobenzene, *J. Chem. Eng. Data.*, **2010**, 55, 4206–4210.
- [24] P. Gupta, T. Agrawal, S. S. Das, N. B. Singh, Phase equilibria and molecular interaction studies on (naphthols + vanillin) systems, *J. Chem. Thermodynamics.*, **2012**, 48, 291–299.
- [25] R. S. B. Reddi, V. S. A. K. Satuluri, U. S. Rai, R. N. Rai, Thermal, physicochemical and microstructural studies of binary organic eutectic systems, *J Therm Anal Calorim.*, **2012**, 107, 377–385.
- [26] N. B. Singh, S. S. Das, P. Gupta, A. Gupta, Phase equilibria and solidification behaviour in the vanillin–p-anisidine system, *J. Cryst. Growth.*, **2008**, 311, 118–122.
- [27] J. Palomar, J.L.G. D. Paz, J. Catalan, Vibrational study of intramolecular hydrogen bonding in *o*-hydroxybenzoyl compounds, *Chemical Physics*. 246 (**1999**) 167–208.
- [28] N. Sundaraganesana, H. Saleem, S. Mohan, Vibrational spectra, assignments and normal coordinate analysis of 2-amino-5-bromopyridine, *Spectrochimica Acta Part A.*, **2003**, 59, 1113–1118.
- [29] M. Singh, R.N. Rai, U.S. Rai, Synthesis, crystal growth and physicochemical studies on a novel organic inter-molecular compound; 3,5-dinitrobenzoic acid and salicylamide system, *J. Cryst. Growth.*, **2015**, 419114–122.
- [30] D. Sinha, A. K. Tiwari, S. Singh, G. Shukla, P. Mishra, H. Chandra, A. K. Mishra, Synthesis, characterization and biological activity of Schiff base analogues of indole-3-carboxaldehyde, *Europ. J. Med. Chem.*, **2008**, 43, 160–165.
- [31] N. R. Desai, R. Khanum, G. Krishnaswamy, R. N. H. Naika, D. B. A. Kumar, S. Sreenivasa. Design, Green Synthesis, Characterization and Antimicrobial Studies of Novel Chalcone Derivatives of Piperazine Substituted Quinolines, *J. Applicable. Chem.* **2016**, 5 (3), 612-619.
- [32] K. Srinivas, P. Raghavaiah, V. Himabindu, G. M. Reddy, B. Balram, Synthesis, Characterization and Crystal Structure of (4-Amino-2-ethoxy-5-nitrophenyl)(piperidin-1-yl) methanone, *J Applicable Chem*, **2014**, 3 (5), 1919-1928.
- [33] H.C. Anitha, S. Sreenivasa1, N.R. Mohan, V. Chandramohan, G. Shivaraja, Preliminary Evaluation of Antimicrobial, Anthelmintic, Anti-Inflammatory Activities and In Silico Studies of Some Cinchoninic Acid Derivatives, *J. Applicable Chem.*, **2017**, 6 (4), 543-558.
- [34] K.S. Thriveni, B. Padmashali, M. B. Siddesh, C. Sandeep, B.C. Goudarshivannanavar, A Facile Synthesis of Piperazine Derivatives and their Pharmacological Profile, *J. Applicable Chem.*, **2013**, 2 (5): 1324-1330.
- [35] M. R. Nadigar, S. Sreenivasa, M. kumar K.E., T Madhu Chakrapani Rao, Synthesis and invitro antibacterial activity of some novel Sulfonamide derivatives bearing 1,4-disubstituted-1,2,4-oxadiazole Moiety, *J. Applicable Chem.*, **2013**, 2 (4), 722-729.

AUTHORS' ADDRESSES

1. **Prof. B. Singh**

Professor, Department of Chemistry, Institute of Science,

B.H.U, Varanasi-221005

E-mail: bsinghbhu@rediffmail.com, Mob. No. 9450546785

2. **Archana Pandey**

Research scholar, Department of Chemistry, Institute of Science,

B.H.U, Varanasi-221005

E-mail: archana.pandey2504@gmail.com, Mob. No. 8765507646